Biochar stimulates the decomposition of simple organic matter and suppresses the decomposition of complex organic matter in sandy loam soil

Cheng, Hongguang; Hill, Paul; Bastami, Mohd Saufi; Jones, David

GCB Bioenergy

Published: 01/06/2017

Publisher's PDF, also known as Version of record

GLOBAL CHANGE BIOLOGY
BIOENERGY

GCB Bioenergy (2017) **9**, 1110–1121, doi: 10.1111/gcbb.12402

Biochar stimulates the decomposition of simple organic matter and suppresses the decomposition of complex organic matter in a sandy loam soil

HONGGUANG CHENG[1,2], PAUL W. HILL[2], MOHD SAUFI BASTAMI[2] and DAVEY L. JONES[2]

[1]*State Key Laboratory of Environmental Geochemistry, Institute of Geochemistry, Chinese Academy of Sciences, Guiyang, Guizhou 550002, China,* [2]*School of Environment, Natural Resources & Geography, Bangor University, Bangor, Gwynedd, LL57 2UW, UK*

Abstract

Incorporating crop residues and biochar has received increasing attention as tools to mitigate atmospheric carbon dioxide (CO_2) emissions and promote soil carbon (C) sequestration. However, direct comparisons between biochar, torrefied biomass, and straw on both labile and recalcitrant soil organic matter (SOM) remain poorly understood. In this study, we explored the impact of biochars produced at different temperatures and torrefied biomass on the simple C substrates (glucose, amino acids), plant residues (*Lolium perenne* L.), and native SOM breakdown in soil using a ^{14}C labeling approach. Torrefied biomass and biochars produced from wheat straw at four contrasting pyrolysis temperatures (250, 350, 450, and 550 °C) were incorporated into a sandy loam soil and their impact on C turnover compared to an unamended soil or one amended with unprocessed straw. Biochar, torrefied biomass, and straw application induced a shift in the soil microbial community size, activity, and structure with the greatest effects in the straw-amended soil. In addition, they also resulted in changes in microbial carbon use efficiency (CUE) leading to more substrate C being partitioned into catabolic processes. While overall the biochar, torrefied biomass, and straw addition increased soil respiration, it reduced the turnover rate of the simple C substrates, plant residues, and native SOM and had no appreciable effect on the turnover rate of the microbial biomass. The negative SOM priming was positively correlated with biochar production temperature. We therefore ascribe the increase in soil CO_2 efflux to biochar-derived C rather than that originating from SOM. In conclusion, the SOM priming magnitude is strongly influenced by both the soil organic C quality and the biochar properties. In comparison with straw, biochar has the greatest potential to promote soil C storage. However, straw and torrefied biomass may have other cobenefits which may make them more suitable as a CO_2 abatement strategy.

Keywords: black carbon, carbon cycling, charcoal, dissolved organic carbon, priming effect, soil management

Received 26 April 2016; accepted 23 August 2016

Introduction

In recent years, conversion of plant biomass to biochar has received increasing attention based on its potential role in mitigating atmospheric CO_2 emissions via sequestering carbon (C) in the soil (Lehmann *et al.*, 2006; Lehmann, 2007). Because of its relative inertness, after amendment, biochar can remain in the soil for hundreds or thousands of years. This contrasts with crop residues (e.g., cereal straw) which turnover on a decadal timescale (Bruun *et al.*, 2008). Thus, biochar created from cereal residues may act as a long-term C sink for offsetting CO_2 emissions (Glaser *et al.*, 2001; Marris, 2006; Lehmann, 2007; Mathews, 2008).

Although C-rich biochar may enhance soil C storage, it is important that it does not destabilize native soil organic matter (SOM) stores or have any other negative environmental consequences if it is to be adopted by policymakers and land owners as a climate change abatement strategy (Jones *et al.*, 2012). This has led to extensive studies on the interactions between natural and anthropogenically derived biochar with both native SOM and plant/animal residues (Wardle *et al.*, 2008; Jones *et al.*, 2011; Luo *et al.*, 2011). Many of these studies have suggested that if the magnitude of any priming effect was considerable (i.e., strong short-term changes in the turnover of SOM caused by comparatively moderate treatment of the soil; Kuzyakov *et al.*, 2000), the

Correspondence: Hongguang Cheng, tel. +86 18984 163868, fax +86 851 85895239, e-mail: chenghongguang@vip.gyig.ac.cn

benefits of C sequestration derived from biochar application into soil would be diminished (Cross & Sohi, 2011). Recent studies have shown both suppression and stimulation of soil organic C (SOC), plant residues, or root exudate decomposition induced by biochar application (Wardle *et al*., 2008; Liang *et al*., 2010; Cross & Sohi, 2011; Jones *et al*., 2011; Luo *et al*., 2011). For example, Wardle *et al.* (2008) reported that the application of black C stimulated SOC decomposition, while Jones *et al.* (2011) observed that it suppressed SOC turnover. It has been suggested that rapid microbial utilization of dissolved or volatile organic C contained in the biochar (Cross & Sohi, 2011), stimulation of microbial activity by changing the chemical environment, and improvements in soil structure and aeration status (Zimmerman, 2010; Jones *et al*., 2011; Smith *et al*., 2011) may account for the observed positive priming effects. In contrast, negative priming effects induced by biochar may be caused by adsorption and subsequent protection of dissolved organic C (DOC) on the surface of the biochar and changes in microbial diversity or in their rate of enzyme production or activity (Dudley & Churchill, 1995; Brändli *et al*., 2008; Koelamans *et al*., 2009). Based on the current uncertainty, we assume that biochar properties, which are controlled by the type of feedstock (Spokas & Reicosky, 2009) and pyrolysis/torrefaction conditions (Yuan *et al*., 2011; Al-Wabel *et al*., 2013; Méndez *et al*., 2013), play an important role in regulating SOM decomposition (Glaser *et al*., 2002; McClellan *et al*., 2007). Changes in pyrolysis temperature, for example, may lead to variations in ash content, porosity, and cation exchange capacity of biochars (Wang *et al*., 2013), which further affects the decomposition of SOM in biochar-amended soils (Yuan *et al*., 2014). However, the direction, magnitude, and temporal dynamics of biochar priming effects on the decomposition of soil C substrates are complex. Further the underlying mechanistic basis of the responses remains poorly understood.

Our objectives were to (i) explore the priming effect of biochar and torrefied biomass application on the decomposition of simple (glucose, amino acids) and complex C substrates (plant residues); (ii) evaluate whether biochar or torrefied biomass alters the turnover of native SOM; (iii) determine which biochar production conditions favor maximal C storage; and (iv) assess the advantages and disadvantages of using straw, and torrefied biomass or biochar as a soil C sequestration agent.

Materials and methods

Feedstock and biochar creation

Biochar was created by the thermal treatment of wheat (*Triticum aestivum* L.) straw, collected from the Henfaes Research Centre Wales, North Wales, UK (53°14′N; 4°10′W). The wheat straw was dried in an oven (80 °C, 24 h) and then cut into 10 cm pieces before being loaded into a glass pyrolysis vessel. The vessel was then placed in a muffle furnace for pyrolysis/torrefaction. The heating rate was 20 °C min^{-1}, and the thermal treatment time was 1 h. Four peak torrefaction/pyrolysis temperatures were set (250, 350, 450, and 550 °C), and the corresponding biochar/torrefaction products were named B_{250}, B_{350}, B_{450}, and B_{550}, respectively. Here, torrefaction is referred to as the low temperature thermal treatment of biomass residues (250 °C) and pyrolysis to high temperature thermal treatment (350–550 °C; Gronnow *et al*., 2013; Bach *et al*., 2016). The main properties of the wheat straw are shown in Table 1.

Soil was collected from the Ah horizon (0–15 cm, sandy loam) of a freely draining, grassland soil (Eutric Cambsiol soil type), which receives regular fertilization (120 kg N, 60 kg K, and 10 kg P annually) and was located at the Henfaes Research Centre. The site is used for both grassland and arable production and has a mean annual temperature of 11 °C (range −5 to 25 °C) and mean annual rainfall of 1060 mm (temperate climate regime). The soil was sieved to pass 5 mm to remove plant residues and stones and then dried at 20 °C prior to use. The major properties of the soil are shown in Table 1 with additional properties shown in Jones *et al.* (2011, 2012) and Farrar *et al.* (2012).

Analysis of soil, straw, and biochar

The ash content of the straw and biochar was measured by heating in a muffle furnace (575 °C, 3 h; Monti *et al*., 2008). Electrical conductivity (EC) and pH were determined in 1 : 5 (w/v) soil : distilled water and 1 : 20 (w/v) biochar : distilled water extracts with standard electrodes. Water holding capacity (WHC) of the biochar and straw was measured according to EBC (2012). Briefly, 2.0 g of biochar or straw was submersed in distilled water for 4 h, then placed on moist sand for 2 h, weighed and subsequently dried (105 °C, 24 h). Cation exchange capacity (CEC) of the biochar and straw was measured using the modified ammonium acetate method of Gaskin

Table 1 Chemical characteristics of the soil and wheat straw used in the experiments

	Soil	Straw
pH	6.44 ± 0.01	6.42 ± 0.16
EC* (μS cm^{-1})	40.9 ± 0.9	1026 ± 47
Total C (g kg^{-1})	21.6 ± 1.85	423 ± 1
Total N (g kg^{-1})	2.62 ± 0.12	5.45 ± 0.05
DOC (mg C kg^{-1})	99.1 ± 1.9	1666 ± 129
K (mg kg^{-1})	77.1 ± 13.1	7816 ± 35
Ca (mg kg^{-1})	735 ± 10	4524 ± 273
Na (mg kg^{-1})	30 ± 2	150 ± 2
NO_3^- (mg N kg^{-1})	10.0 ± 0.4	0.66 ± 0.08
NH_4^+ (mg N kg^{-1})	4.7 ± 0.4	14.8 ± 0.9

Values represent means ± standard error of the mean (SEM), n = 4.

*Electrical conductivity.

et al. (2008). Specific surface area (SSA) of the biochar and straw was measured using an Autosorb iQ/monosorb surface area analyzer (Quantachrome Instruments, Boynton Beach, FL, USA), with N_2 absorption at 77 K, using the Brunauer–Emmett–Teller method. Available NO_3^- and NH_4^+ were determined in 0.5 M K_2SO_4 extracts (1 : 5 w/v) using the colorimetric methods of Mulvaney (1996) and Miranda *et al.* (2001). Exchangeable cations and available phosphorous (P) were extracted using 0.5 M acetic acid (1 : 5 w/v) and analyzed through a Model 410 Flame Photometer for Na, K, and Ca and the colorimetric molybdate blue method for P (Murphy & Riley, 1962).

Experimental treatments

The experiments had six main treatments: (i) unamended soil (control), (ii) straw-amended soil, (iii) B_{250} amended soil, (iv) B_{350} amended soil, (v) B_{450} amended soil, and (vi) B_{550} amended soil. Biochar and straw were added to soil at a soil-to-residue ratio of 10 : 1 (w/w). The addition rates were based on the likely maximal addition rates of biochar in an agricultural topsoil (0–10 cm) and those used in previous field trials at the site (Jones *et al.*, 2012). Wheat straw was chosen as it represents the major cereal waste produced in the UK and crop residue incorporated into soil (12.2×10^6 t yr^{-1} at ca. 3.5 t ha^{-1} yr^{-1}; Defra, 2014). The straw addition rates are higher than those typically applied by farmers when averaged across a field, but reflect the hotspots of straw which frequently occur in topsoils after residue incorporation. All treatments were performed in quadruplicate.

Basal soil respiration

Briefly, 20 g of air-dried soil and 2 g of biochar or straw were mixed, the water content adjusted to 32% with distilled water and the samples placed in 50 cm^3 sterile polypropylene tubes. Soil respiration was then measured over a 168-h period at 20 °C using an automated multichannel SR1-IRGA soil respirometer (PP Systems Inc., Hitchin, UK).

Mineralization of simple ^{14}C-labeled C substrates

Two ^{14}C-labeled simple C substrates and two ^{14}C-labeled complex C substrates were used to determine the impact of biochar and straw on microbial SOC turnover. Glucose and free amino acids were chosen to simulate low molecular weight (MW) root exudates (simple substrates), and plant shoot residues (*Lolium perenne* L.) and aged SOM were chosen to simulate more complex high MW C substrates.

Soil (10 g, 32% moisture content) from each of the six experimental treatments was placed into sterile 50-cm^3 polypropylene tubes. The tubes were then amended with 0.5 mL of either ^{14}C-labeled glucose (36 mg C g^{-1} soil; 1.26 kBq mL^{-1}) or an equimolar mixture of 16 amino acids (31.2 mg C g^{-1} soil; 1.38 kBq mL^{-1}) (Jones *et al.*, 2012). A vial containing 1 mL of 1 M NaOH was then placed above the samples to trap any $^{14}CO_2$ evolved and the centrifuge tubes hermetically sealed. Samples were then placed in a climate-controlled room (20 °C) and the NaOH traps changed periodically over 21 days. The $^{14}CO_2$ content in the NaOH traps was determined by liquid scintillation counting using Optiphase 3 scintillation fluid (PerkinElmer Corp., Waltham, MA, USA) and a Wallac 1404 liquid scintillation counter (PerkinElmer Corp.).

Mineralization of complex ^{14}C-labeled C substrates

The ^{14}C-labeled soil and plant residues were obtained from the same site used to collect the unlabeled soil. Briefly, steel frames were placed into the *L. perenne* L. grass swards. Acrylic chambers (15 × 30 cm, height 60 cm) were then clamped onto the frames and 7.4 MBq $NaH^{14}CO_3$ injected into a reaction vessel containing dilute HCl to generate $^{14}CO_2$. The chambers were then sealed for 1 h and the headspace continuously mixed using a battery-powered fan (Hill *et al.*, 2007). The chamber was then removed and the ^{14}C-labeled shoot material harvested after 6 days, air-dried and stored at 20 °C in a sealed container. Six years after ^{14}C labeling the swards, soil was recovered (0–10 cm depth) from the plots. This was considered to contain quasi-stable ^{14}C-labeled SOM based on the C dynamics of this site (see Farrar *et al.*, 2012; Hill *et al.*, 2015).

As described for the simple C substrates, ^{14}C-labeled *L. perenne* shoots (100 mg; 12.7 kBq g^{-1}) were mixed with 10 g of soil for each of the six treatments. $^{14}CO_2$ evolution was then determined over 21 days. Due to the lower specific activity of the ^{14}C-labeled SOM, 100 g of ^{14}C-labeled soil was mixed with biochar or straw in a 500 cm^3 glass vessel similar to that described previously except that larger (4 mL) 1 M NaOH traps were used and $^{14}CO_2$ evolution measured over 105 days.

Dissolved organic carbon dynamics

Soil (1 kg) from each of the six treatments was placed in plastic containers (135 × 102 × 283 mm) and incubated at 70% relative humidity and 20 °C for 60 days. During incubation, soil solutions were recovered nondestructively with 5-cm-long Rhizon® soil solution samplers (Rhizosphere Research Products B.V., Wageningen, the Netherlands). Dissolved organic C (DOC) and total dissolved N (TDN) in soil solution were determined using a Multi N/C 2100 analyzer (Analytik Jena, Jena, Germany). Dissolved organic and dissolved N (NH_4^+ and NO_3^-) in soil solution were determined using a Multi N/C 2100 analyzer (Analytik Jena, Jena, Germany) and using the colorimetric methods of Mulvaney (1996) and Miranda *et al.* (2001), respectively.

Microbial biomass and community structure

At the end of the incubation experiment, soil (20 g) from the 1 kg containers was collected for phospholipid fatty acid (PLFA) profiling and for microbial biomass C and N determination. Following Buyer & Sasser (2012), soil from each treatment was freeze-dried (2 g) and 4 mL of Bligh-Dyer extractant containing an internal standard added. The samples were then sonicated (10 min, 20 °C), rotated end-over-end (2 h), and centrifuged (10 min). The liquid phase was transferred into clean screw-cap test tubes (13 × 100 mm) and 0.1 mL of chloroform and water added. The upper phase was discarded, whilst the lower phase containing the extracted lipids was evaporated at 30 °C. Solid phase extraction using a 96-well SPE plate containing 50 mg of silica per well (Phenomenex Inc., Torrance, CA, USA) was used to separate lipids. Each sample was allowed to evaporate in a glass vial (30 min, 70 °C) with 0.5 mL of 5 : 5 : 1 methanol: chloroform: H_2O; the latter process was performed for eluting phospholipids. After evaporation, a transesterification reagent (0.2 mL) was added to each vial, after which the vials were sealed and incubated (37 °C, 15 min). Acetic acid (0.075 M) and chloroform (0.4 mL) were added to each vial; chloroform was evaporated just to dryness and the samples dissolved in hexane. Measurements were performed on a 6890 gas chromatograph (Agilent Technologies, Wilmington, DE, USA) equipped with an autosampler, split–splitless inlet, and flame ionization detector. Fatty acid methyl esters (FAMEs) were separated on an Agilent Ultra 2 column, 25 m long × 0.2 mm internal diameter × 0.33 μm film thickness. Different taxonomic groups were classified as described in Frostegård *et al.* (1993) with acknowledgment of the caveats raised in Frostegård *et al.* (2011).

As for PLFA analysis, soil samples were collected after 60 days. Microbial biomass C and N (MBC and MBN) were determined based on the of $CHCl_3$ fumigation-K_2SO_4 extraction method of Joergensen *et al.* (2011). After fumigation, DOC and TDN in the 0.5 M K_2SO_4 extracts were determined as described above. MBC was calculated using the standard conversion factor (K_{ec}) of 0.45, while for MBN, a K_{en} value of 0.54 was used (Brookes *et al.*, 1985; Wu *et al.*, 1990).

Kinetic modeling of ^{14}C-labeled glucose and amino acid mineralization in soil

Many earlier studies have indicated that the mineralization of simple ^{14}C-labeled organic substrates such as those used here (e.g., amino acids and sugars) follow a biphasic kinetic pattern (Hill *et al.*, 2008, 2012; Farrar *et al.*, 2012; Oburger *et al.*, 2012). A kinetic model was therefore fitted to the experimental data to provide information on the internal use of the ^{14}C by the soil microbial community. Specifically, the model allows ^{14}C taken up by the microbial biomass to be partitioned into that used for respiration (catabolic processes) and that used to make new cell biomass (anabolic processes) (Glanville *et al.*, 2016).

Following Glanville *et al.* (2016), a double exponential first-order kinetic decay model was fitted to the ^{14}C-glucose and ^{14}C-amino acid mineralization data. Firstly, the data were transformed to reflect the amount of ^{14}C remaining in the soil over time (rather than the amount lost from the soil as shown in Fig. 2). The following kinetic equation was then fitted to the data where

$$Y = [a_1 \times \exp^{(-k_1 t)}] + [a_2 \times \exp^{(-k_2 t)}] \quad (1)$$

and where Y represents the amount of ^{14}C remaining in the soil, a_1 describes the amount of ^{14}C partitioned into the first rapid mineralization pool (*C pool 1*), k_1 is the exponential decay coefficient for *C pool 1*, while a_2 describes the second slower mineralization pool (*C pool 2*), and k_2 is the exponential decay coefficient for *C pool 2*, and t is time after ^{14}C-substrate addition to soil. *C pool 1* was attributed to the rapid use of ^{14}C substrate in catabolic processes leading to the loss of $^{14}CO_2$ in respiration, while *C pool 2* was attributed to the slower turnover of ^{14}C, assumed to be initially immobilized in the microbial biomass via anabolic processes. The assumptions and validation of this modeling approach are provided in Glanville *et al.* (2016). The half-life period ($t_{½}$) for the first mineralization pool (*C pool 1*) can be calculated using the following equation:

$$t_{1/2} = \ln(2)/k_1 \quad (2)$$

However, the added C substrate to soil may be transformed by several microbial processes, and calculating the half-life period for the second phase (*C pool 2*, k_2) is subject to uncertainty due to the complexity over the connectivity between pool *C pool 1* and *C pool 2* (Boddy *et al.*, 2008; Glanville *et al.*, 2016).

Following Glanville *et al.* (2016), the microbial carbon use efficiency (CUE) for the ^{14}C-labeled substrates was calculated as follows:

$$\mathrm{CUE} = C\,pool\,2/(C\,pool\,1 + C\,pool\,2) \quad (3)$$

A least sum of squares curve fitting algorithm in SIGMAPLOT v12.3 (Systat Software Inc., San Jose, CA, USA) was used to fit the kinetic equation to the experimental data (Glanville *et al.*, 2016).

Statistical analyses

Statistical analyses were carried out using SPSS v19.0 (SPSS Inc., Chicago, IL, USA). A one-way analysis of variance followed by a least significant difference test was used to determine significant differences (cutoff value of 95%) between treatments. Linear regression was undertaken in SIGMAPLOT v12.5 (Systat Software Inc.).

Results

Analysis of biochar properties

As the torrefaction/pyrolysis temperature increased, biochar pH, specific surface area and water holding capacity significantly increased (Table 2). In contrast, biochar EC and CEC decreased with increasing temperature. Soluble C in the biochar exhibited a different pattern being maximal at an intermediate heating temperature (350 °C) and then declining markedly at the higher thermal regimes.

Soil respiration

Compared to the unamended soil (79 μmol CO_2 kg^{-1}), soil respiration was significantly higher in the biochar or straw-amended soils ($P < 0.001$; Fig. 1). Overall, the straw-amended soil showed the highest CO_2 emission being 5–10 times higher than in the different biochar treatments. In the biochar-amended soils, the highest pyrolytic temperatures had significantly lower CO_2

Table 2 Physical and chemical properties of torrefied biomass produced at 250 °C (B_{250}) and biochar produced at either 350 °C (B_{350}), 450 °C (B_{450}), or 550 °C (B_{550})

	B_{250}	B_{350}	B_{450}	B_{550}
pH	5.40 ± 0.08^{d}	8.84 ± 0.10^{c}	9.19 ± 0.10^{b}	9.74 ± 0.17^{a}
EC ($\mu S\ cm^{-1}$)	3355 ± 125^{d}	1825 ± 158^{c}	1384 ± 39^{b}	1242 ± 77^{a}
SSA ($m^2\ g^{-1}$)	2.70 ± 0.01^{d}	5.20 ± 0.01^{c}	4.55 ± 0.01^{b}	10.5 ± 0.01^{a}
CEC ($cmol\ kg^{-1}$)	68.7 ± 0.5^{d}	58.6 ± 1.7^{c}	40.5 ± 1.2^{b}	22.0 ± 1.3^{a}
WHC (%)	275 ± 11^{b}	333 ± 23^{a}	355 ± 34^{a}	339 ± 12^{a}
DOC ($mg\ kg^{-1}$)	1430 ± 90^{d}	1990 ± 140^{c}	1010 ± 20^{b}	560 ± 60^{a}

EC, electrical conductivity; SSA, specific surface area; CEC, cation exchange capacity; WHC, water holding capacity; DOC, dissolved organic carbon.
All values represent means ± SEM (n = 4). Different superscript letters represent significant differences between treatments at the $P < 0.05$ level.

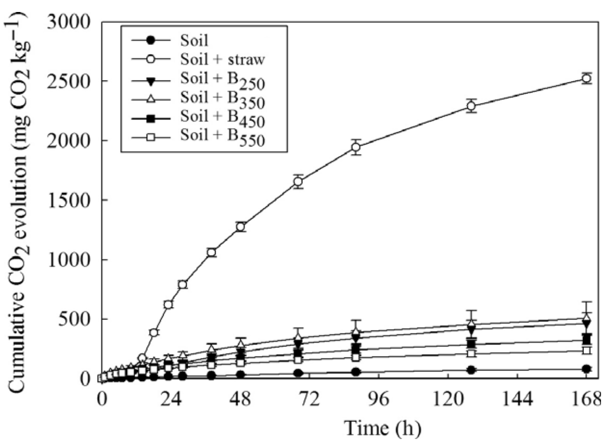

Fig. 1 Influence of untreated straw, torrefied biomass produced at 250 °C (B_{250}) and biochar produced at either 350 °C (B_{350}), 450 °C (B_{450}), or 550 °C (B_{550}) on cumulative CO_2 evolution from an agricultural soil. Data points represent means ± SEM (n = 4).

emissions; however, these were still higher than in the soil-only control treatment.

Mineralization of simple ^{14}C-labeled substrates

The slowest ^{14}C-glucose mineralization rate occurred in the unamended soil treatment ($P < 0.001$; Fig. 2a). Among the biochar-amended soils, the highest substrate mineralization rates were observed in the treatments containing biochar produced at lower temperatures. Biochar produced at 550 °C initially repressed glucose mineralization in comparison with the control; however, after 21 days, the amount of $^{14}CO_2$ produced was not significantly different from the soil-only treatment. In comparison with biochar, the addition of straw greatly stimulated substrate mineralization particularly during the first 48 h; however, the subsequent rate of $^{14}CO_2$ evolution after this initial mineralization phase was similar to the control.

A similar trend to that observed for ^{14}C-glucose was also seen for the effect of biochar and straw on the mineralization of amino acids in soil (Fig. 2b). The lowest amount of mineralization was seen in the unamended soil and the soil amended with biochar produced at the highest pyrolytic temperature. The greatest stimulation of mineralization of the amino acid mixture was again in the soil amended with straw and biochar produced at the lowest temperature.

Kinetic modeling of ^{14}C-labeled glucose and amino acid mineralization in soil

Overall, the double exponential kinetic model fitted well to the experimental data. The average r^2 value describing the closeness of fit of the model to the experimental data across all six treatments was 0.992 ± 0.002 for glucose and 0.993 ± 0.002 for the amino acid mixture (Tables 3 and 4). For ^{14}C-glucose, most of the ^{14}C was initially immobilized in the microbial biomass (*C pool 2*) with only a small amount immediately used in energy production (*C pool 1*). The presence of straw in the soil shifted the partitioning of C within the cell, with proportionally more ^{14}C allocated to rapid energy production. Overall, the presence of biochar shifted C partitioning within the microbial community, particularly in the presence of torrefied biomass and low temperature biochars (B_{250}, B_{350}). This resulted in a significant alteration of microbial CUE. The presence of the chars produced at high temperatures also repressed the initial mineralization of glucose as evidenced by the increase in half-life associated with *C pool 1*. The lower rate constant (k_2) values for *C pool 2* may possibly suggest that biochars produced at high temperature marginally suppress the turnover of ^{14}C immobilized in the microbial biomass. The turnover of this C pool equates to the turnover of the microbial biomass during both cell maintenance and also due to death of cells and

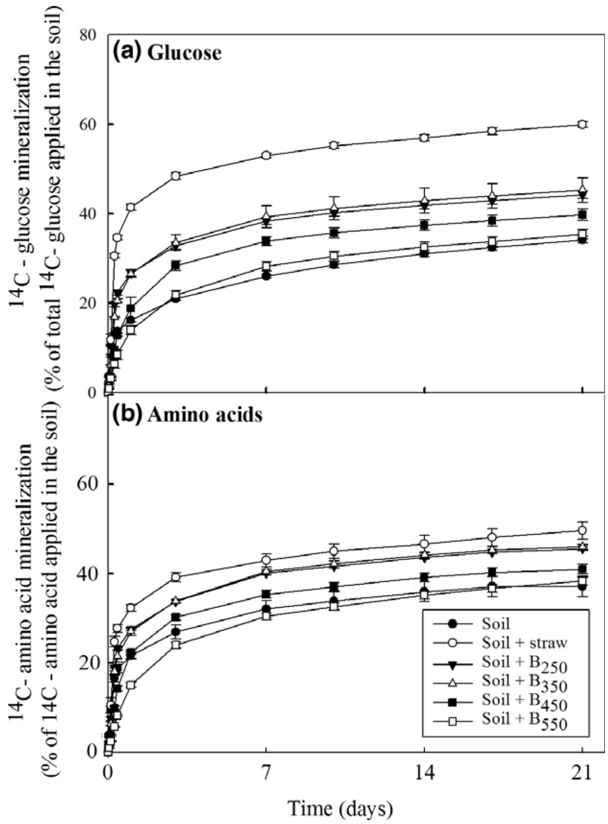

Fig. 2 Influence of untreated straw, straw-derived torrefied biomass produced at 250 °C (B_{250}) and biochar produced at either 350 °C (B_{350}), 450 °C (B_{450}), or 550 °C (B_{550}) on the mineralization of either ^{14}C-glucose (panel a) or ^{14}C-amino acids (panel b) in an agricultural soil. Values represent means ± SEM (n = 4). The legend is the same for both panels.

subsequent extracellular (i.e., by exoenzymes) or intracellular (e.g., by protozoal ingestion) breakdown of the C in the microbial cells and use of the C released by other organisms (Glanville *et al.*, 2016).

Kinetic modeling of the ^{14}C-labeled amino acids through the microbial biomass revealed very similar results to those obtained for ^{14}C-glucose. Overall, both straw and torrefied biomass promoted the allocation of more C toward catabolic processes resulting in lower CUE values in comparison with the unamended control. In addition, high temperature chars repressed the rate of amino acid-C flow through *C pool 1* relative to the control. Biochar did not appear to alter the rate of amino acid-derived C processed through the microbial biomass (k_2, *C pool 2*).

Mineralization of ^{14}C-labeled native SOM and plant residues

The highest rate of ^{14}C-SOM mineralization was seen in the straw-amended soil (Fig. 3a). However, although biochar produced at the two lowest pyrolysis temperatures initially stimulated SOC mineralization, after 60 days, all biochar amendments had significantly reduced SOC mineralization relative to the unamended soil (P < 0.001).

Although the results were variable, in contrast to other ^{14}C-labeled substrates, the mineralization of the plant residues was suppressed by all amendments, including straw. However, in common with other substrates, the greatest suppression was seen in the treatment containing biochars produced at high temperatures (Fig. 3b).

Microbial biomass and community structure

Phospholipid fatty acid analysis, MBC and MBN were used to determine whether biochar or straw affected the microbial community structure and abundance. Compared to the unamended control treatment, the abundance of Gram-negative bacteria and fungi in the biochar-amended soils was higher, whereas the abundance of Gram-positive bacteria and anaerobes was significantly lower. In biochar-amended soils, an increase of pyrolytic temperatures was associated with a decrease of Gram-negative bacteria and fungi; in contrast, it was associated with an increase of Gram-positive bacteria and anaerobes (Table 5), and higher MBC and MBN (Table 6). Nevertheless, compared to the unamended soil, MBC and MBN were significantly higher in the biochar-amended soils. In addition, higher DOC concentrations were observed in the biochar-amended soil solutions, although these tended to decrease in the presence of chars produced at higher temperatures (Fig. 4).

Soluble N concentrations were dominated by NO_3^- and decreased in all treatments over time (Fig. 5). Overall, the concentrations of NH_4^+ declined to very low levels in all treatments after 7 days although the most rapid decline was seen in the straw treatment. In contrast to the unamended control treatment, NO_3^- concentrations remained extremely, low in the presence of straw throughout the 60-day monitoring period. Generally, the presence of biochar resulted in an initial increase in NO_3^- concentration; however, the concentration then progressively declined until almost no NO_3^- remained in solution by 60 days. The decline in NO_3^- was most apparent in the high temperature chars. The average (±SEM) total soluble inorganic N concentrations in the different treatments over the 60-day incubation period were 136 ± 11 mg N L^{-1} (control), 0.4 ± 0.1 mg N L^{-1} (straw), 50 ± 9 mg N L^{-1} (B_{250}), 45 ± 8 mg N L^{-1} (B_{350}), 32 ± 7 mg N L^{-1} (B_{450}), and 22 ± 8 mg N L^{-1} (B_{550}).

Table 3 Influence of straw, torrefied biomass produced at 250 °C (B_{250}), and biochar produced at either 350 °C (B_{350}), 450 °C (B_{450}), or 550 °C (B_{550}) on the partitioning and rate of flux of glucose-derived ^{14}C through the soil microbial biomass

			Biochar			
	Control	Straw	B_{250}	B_{350}	B_{450}	B_{550}
C pool 1 (% of total)	16.6 ± 1.8	47.6 ± 1.9	31.6 ± 2.0	32.9 ± 1.9	28.7 ± 1.4	22.6 ± 1.2
C pool 2 (% of total)	82.7 ± 1.3	54.5 ± 2.4	69.3 ± 1.6	67.8 ± 1.6	71.1 ± 1.3	76.8 ± 1.1
k_1 (day^{-1})	4.73 ± 1.32	3.31 ± 0.412	2.98 ± 0.47	2.20 ± 0.31	1.13 ± 0.14	0.83 ± 0.11
k_2 (day^{-1})	0.012 ± 0.001	0.016 ± 0.003	0.012 ± 0.002	0.012 ± 0.002	0.009 ± 0.001	0.009 ± 0.001
C pool 1 half-life (day)	0.15	0.21	0.23	0.32	0.61	0.83
C use efficiency (CUE)	0.83	0.53	0.69	0.67	0.71	0.77
Model r^2	0.983	0.993	0.990	0.993	0.996	0.997

The size of *C pool 1* and *C pool 2* represent the total amount of ^{14}C initially assigned to catabolic and anabolic processes, respectively, within the cell. The decay constants k_1 and k_2 are the rates for pools *C pool 1* and *C pool 2*, respectively. Values represent mean ± SEM. The model r^2 value describes the fit of the kinetic model (Eqn 1) to the experimental data.

Table 4 Influence of straw, torrefied biomass produced at 250 °C (B_{250}) and biochar produced at either 350 °C (B_{350}), 450 °C (B_{450}), or 550 °C (B_{550}) on the partitioning and rate of flux of amino acid-derived ^{14}C through the soil microbial biomass

			Biochar			
	Control	Straw	B_{250}	B_{350}	B_{450}	B_{550}
C pool 1 (% of total)	24.2 ± 1.8	36.7 ± 1.9	32.2 ± 2.1	33.0 ± 2.2	30.5 ± 1.1	25.2 ± 0.8
C pool 2 (% of total)	75.3 ± 1.4	63.9 ± 1.4	67.9 ± 1.7	67.4 ± 1.8	69.7 ± 1.0	74.7 ± 0.8
k_1 (day^{-1})	3.33 ± 0.63	3.37 ± 0.43	2.67 ± 0.43	2.31 ± 0.38	1.33 ± 0.12	0.79 ± 0.06
k_2 (day^{-1})	0.010 ± 0.002	0.012 ± 0.002	0.012 ± 0.002	0.012 ± 0.002	0.009 ± 0.001	0.010 ± 0.001
C pool 1 half-life (day)	0.21	0.21	0.26	0.30	0.52	0.87
C use efficiency (CUE)	0.76	0.63	0.68	0.67	0.70	0.75
Model r^2	0.987	0.992	0.990	0.990	0.997	0.999

The size of *C pool 1* and *C pool 2* represents the total amount of ^{14}C initially assigned to catabolic and anabolic processes, respectively, within the cell. The decay constants k_1 and k_2 are the rates for pools *C pool 1* and *C pool 2*, respectively. Values represent mean ± SEM. The model r^2 value describes the fit of the kinetic model (Eqn 1) to the experimental data.

Discussion

Impact of straw and biochar on soil respiration

The results presented here clearly show that the addition of biochar to soil increased basal respiration, albeit to a much lesser extent than observed in the presence of straw. The addition of straw was characterized by a short lag phase in CO_2 efflux, which presumably reflects the adaptation and growth of the microbial biomass in response to the addition of a large amount of labile C (Cayuela *et al.*, 2009). This is supported by the observed increase in microbial biomass during the experiment. In contrast, no lag phase in soil respiration was apparent in the biochar treatments suggesting a lack of rapid microbial growth; however, all the biochars increased CO_2 emissions relative to the control. While this response could be attributed to the positive priming of native SOM, it can also be attributable to the loss of C from the biochar itself. Using the same soil, Jones *et al.* (2011) showed that the increase in soil respiration after the addition of a wood-based biochar was partially due to the biotic breakdown of DOC contained in the biochar and from the abiotic release of CO_2 from biochar minerals formed during pyrolysis. In our study, the stimulation in soil respiration was positively correlated with biochar DOC content (r^2 = 0.935). The amount of DOC added to the soil in the biochar (56–199 mg C kg^{-1}), however, was lower than the additional amount of CO_2 produced from the biochar-soil mixtures over 7 days (154–386 mg C kg^{-1}), relative to the control. It also cannot account for the increase in MBC in soil upon biochar addition (82–286 mg C kg^{-1}). This suggests that biochar-derived DOC alone cannot account for the observed increase in CO_2. It is also unlikely that abiotic CO_2 release can explain this increase as the contribution from this source would be expected to increase with biochar production temperature (as the C-to-mineral ratio decreases and more metal oxides are formed; Angin, 2013). The additional CO_2 could

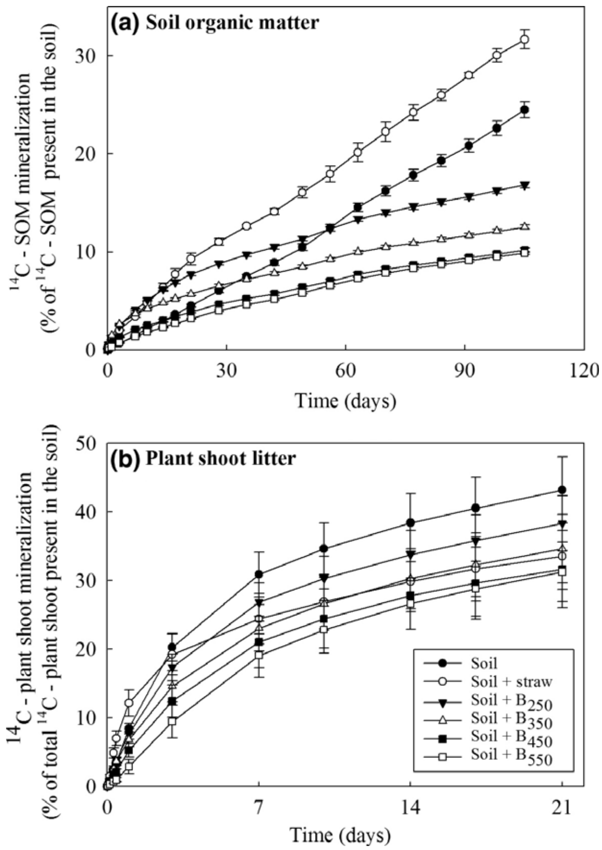

Fig. 3 Influence of untreated straw, straw-derived torrefied biomass produced at 250 °C (B_{250}) and biochar produced at either 350 °C (B_{350}), 450 °C (B_{450}), or 550 °C (B_{550}) on the mineralization of either ^{14}C-labeled native soil organic matter (panel a) or ^{14}C-labeled plant shoot litter (panel b) in an agricultural soil. Values represent means ± SEM (n = 4). The legend is the same for both panels.

therefore originate from native SOC (i.e., positive priming) or from the microbial-induced solubilization and breakdown of the biochar (Jiang *et al.*, 2016).

Table 6 Influence of adding untreated straw and straw-derived torrefied biomass produced at 250 °C (B_{250}) and biochar produced at either 350 °C (B_{350}), 450 °C (B_{450}), or 550 °C (B_{550}) on soil microbial biomass carbon (MBC) and nitrogen (MBN)

Treatment	MBC (mg C kg^{-1})	MBN (mg N kg^{-1})
Soil	635 ± 8^{e}	40 ± 2^{c}
Straw	1843 ± 127^{a}	160 ± 14^{a}
B_{250}	717 ± 17^{d}	31 ± 2^{d}
B_{350}	803 ± 45^{c}	44 ± 5^{c}
B_{450}	897 ± 20^{b}	43 ± 7^{bc}
B_{550}	921 ± 33^{b}	52 ± 3^{b}

Values represent means ± SEM (n = 4). Different superscript letters represent significant differences between treatments at the $P < 0.05$ level.

Positive priming effects of biochar

Based on our ^{14}C-labeled SOM experiment, biochars produced at lower temperatures initially accelerated native SOM turnover by twofold to threefold within the first 7 days, suggesting that this may also account for some of the additional CO_2 produced immediately after biochar addition. This positive priming, however, was short-lived and is unlikely to be of concern in terms of the net C balance of the soil in the longer term.

In this study, biochar application generally appeared to stimulate the mineralization of the simple C substrates, glucose, and amino acids. This was surprising as their mineralization is typically insensitive to major changes in soil management (Jones *et al.*, 2005). A number of factors may explain the apparent stimulation of simple C substrate turnover including: (i) inputs of DOC from the biochar may promote general microbial activity in the soil leading to faster uptake rates and mineralization (De Nobili *et al.*, 2001; Hamer *et al.*, 2004), (ii) the biochar may absorb humic substances

Table 5 Influence of adding untreated straw and straw-derived torrefied biomass produced at 250 °C (B_{250}) and biochar produced at either 350 °C (B_{350}), 450 °C (B_{450}), or 550 °C (B_{550}) to soil on the relative abundance of microbial groups determined by PLFA profiling

Group	Control	Straw	B_{250}	B_{350}	B_{450}	B_{550}
Gram+ bacteria	27.3 ± 0.2^{d}	23.9 ± 0.5^{a}	25.1 ± 0.1^{b}	24.6 ± 0.3^{c}	24.1 ± 0.2^{c}	25.3 ± 0.3^{b}
Gram− bacteria	46.1 ± 0.2^{e}	50.8 ± 0.7^{a}	49.6 ± 0.1^{d}	48.2 ± 0.4^{c}	49.1 ± 0.8^{cd}	47.6 ± 0.2^{b}
Fungi	1.6 ± 0.1^{c}	7.1 ± 0.2^{a}	2.8 ± 0.5^{b}	3.0 ± 0.4^{b}	3.3 ± 0.7^{b}	3.3 ± 0.6^{b}
AMF	4.6 ± 0.1^{b}	4.2 ± 0.1^{a}	3.9 ± 0.1^{d}	4.3 ± 0.1^{ac}	4.4 ± 0.1^{c}	4.7 ± 0.2^{b}
Actinomycetes	16.8 ± 0.2^{c}	9.6 ± 0.2^{a}	15.6 ± 0.2^{b}	16.5 ± 0.3^{c}	15.5 ± 0.2^{b}	15.2 ± 0.6^{b}
Anaerobes	1.3 ± 0.1^{c}	0.9 ± 0.0^{a}	1.0 ± 0.1^{b}	1.1 ± 0.1^{b}	1.0 ± 0.2^{ab}	0.9 ± 0.1^{ab}
Eukaryotes	2.4 ± 0.3^{bc}	3.4 ± 0.2^{a}	2.0 ± 0.2^{c}	2.4 ± 0.1^{b}	2.6 ± 0.4^{b}	2.9 ± 0.4^{ab}

Gram+, Gram positive; Gram−, Gram negative; AMF, Putative arbuscular mycorrhizal fungi.
Values represent means ± SEM (n = 4). Different superscript letters represent significant differences between treatments at the $P < 0.05$ level.

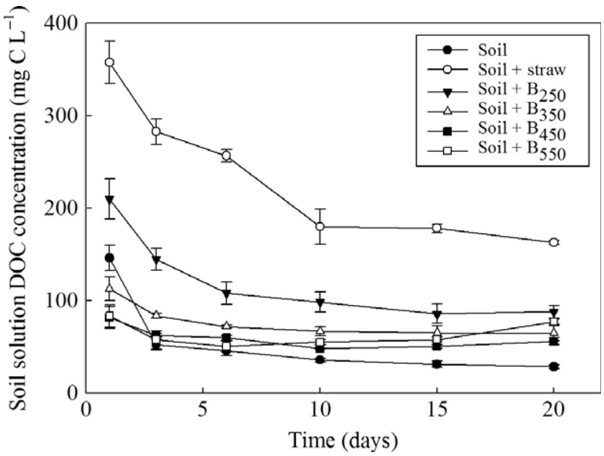

Fig. 4 Influence of adding untreated straw and straw-derived torrefied biomass produced at 250 °C (B_{250}) and biochar produced at either 350 °C (B_{350}), 450 °C (B_{450}), or 550 °C (B_{550}) on soil solution dissolved organic carbon (DOC) concentration over a 21 days period. Values represent means ± SEM (n = 4).

from soil solution which previously limited microbial activity (Ni *et al.*, 2011), (iii) the biochar is inducing growth of the microbial community leading to a greater C sink, or (iv) biochar is influencing the internal partitioning of C within the microbial cell (immobilization-to-mineralization ratio) and thus microbial C use efficiency (CUE) (Farrell *et al.*, 2015). Unlike previous studies (Riedel *et al.*, 2014), our soil solution data do not lend support to hypothesis (ii). Although we present some evidence to support hypotheses (i) and (iii), the patterns of CO_2 evolution suggest to us that hypothesis (iv) is the most likely explanation.

If biochar was alleviating stress in the microbial community (e.g., by absorbing toxic metals or xenobiotics), we would expect CUE to increase as less C is invested in energy-intensive stress avoidance strategies (Tiemann & Billings, 2011). However, the kinetic modeling undertaken here clearly suggests that biochar addition decreases microbial CUE, particularly in the presence of low temperature chars. This result contrasts with Jiang *et al.* (2016) where an increased CUE was observed in the presence of biochar. The consistently reduced CUE for the C substrates studied here could be attributable to shifts in microbial community structure, to reductions in N availability, or to shifts in available C within the soil. The largest reduction in CUE was observed in the straw treatment (C : N ratio = 77), consistent with N limitation within the microbial community and an increase in overflow respiration (Sinsabaugh *et al.*, 2013; Spohn *et al.*, 2016). In support of this N limitation hypothesis, biochar is known to readily adsorb soluble N (Jones *et al.*, 2011; Subedi *et al.*, 2015; Tian *et al.*, 2016), potentially limiting its availability to the soil microbial community. This sorption was expected to be

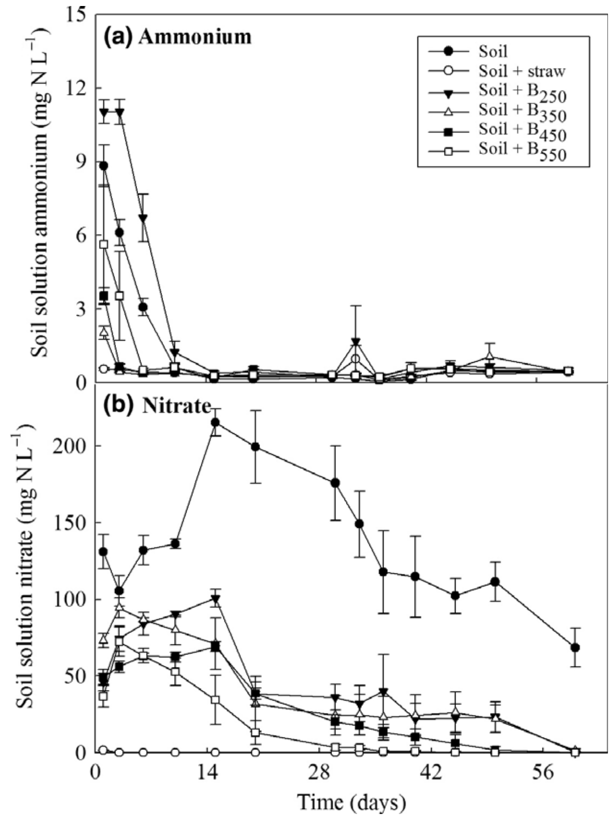

Fig. 5 Influence of adding untreated straw and straw-derived torrefied biomass produced at 250 °C (B_{250}) and biochar produced at either 350 °C (B_{350}), 450 °C (B_{450}), or 550 °C (B_{550}) on soil solution nitrate and ammonium concentrations over a 60-day period. Values represent means ± SEM (n = 4).

especially prevalent in biochars with a high CEC where the lowest CUE values were obtained. However, CEC was not correlated with the rate of disappearance of either NH_4^+ or NO_3^- from soil solution, suggesting that this may not wholly explain our CUE results. Alternatively, DOC originating from the biochar may be preferred by the microbial community for catabolic processes, thereby freeing up a greater use of glucose and keto acids (produced from amino acid deamination) for use in respiratory pathways. Microbial community composition has also been hypothesized to influence CUE. In our study, we observed an increase in fungal biomass; however, increases in fungal-to-bacterial ratio are typically associated with an increase in CUE rather than a decrease as observed here (Keiblinger *et al.*, 2010).

Overall, our results initially suggested that biochar accelerated low MW C turnover in soil. Closer examination of the results using kinetic modeling, however, actually revealed slower rates of turnover in the presence of biochar. This was associated with a major shift in microbial CUE which we attribute to the reduced availability of N and the increased presence of alternative C substrates in solution.

Negative priming effect of biochar on native SOM

Although biochar application initially stimulated native SOM turnover, in the longer term, it significantly reduced SOM and plant residue turnover, consistent with the findings of previous studies in the same soil (Jones *et al*., 2012) and in the meta-analyses undertaken by Maestrini *et al*. (2015) and Wang *et al*. (2016). Lu *et al*. (2014) also observed that biochar application suppressed SOC decomposition, whereas the co-addition of inorganic N stimulated it. Although Lu *et al*. (2014) hypothesized that the decrease in SOC decomposition was mainly due to the sorption of DOC by biochars, a range of factors could be responsible for the negative priming response observed here (Rittl *et al*., 2015a). While N limitation could repress microbial activity, it frequently leads to the positive priming of soil organic matter, suggesting that this is probably not the mechanism (Murphy *et al*., 2015). The results from the kinetic modeling presented here (*C pool 2*, k_2) and in Jones *et al*. (2012) also suggest that biochar does not greatly alter the rate of turnover of C contained in the soil microbial biomass. Therefore, it is more likely that the negative priming is associated with the microbial community switching to an alternative source of C. This could be derived from the biochar itself or include a pool of SOM which was not heavily ^{14}C-labeled. In support of the first theory, the observed reduction in soil solution DOC over time certainly suggests that the microbial community is utilizing an alternative C source. This is supported by the results of Jones *et al*. (2011) who showed that wood-derived biochar DOC could be rapidly respired by the soil microbial community.

Influence of biochar properties on the priming effect

Consistent with previous studies, our results showed that higher pyrolytic temperatures led to increases in specific surface area and moisture retention while decreasing CEC and DOC content (Mukherjee *et al*., 2011; Wang *et al*., 2013). The characteristics of these high temperature biochars promoted greater negative priming of SOM in our study, and they have recently been advocated as the best type of char for maximizing soil C storage (Yuan *et al*., 2014). However, increasing amounts of C are also volatilized during the production of biochar at higher pyrolysis temperatures (Lehmann *et al*., 2006), so ultimately less C per unit mass of feedstock is available for soil incorporation. In addition, some of the beneficial properties of the biochar may be lost (i.e., its ability to retain nutrients and moisture). Therefore, even though low temperature chars and torrefied biomass do not provide the optimal conditions for SOM stabilization, the greater volume of C available to add to the soil may offset this.

It has been proposed that the addition of crop residues to soil may promote the loss of SOM (Fontaine *et al*., 2004). In partial agreement with this, our study demonstrated that straw promoted the positive priming of native SOM; however, it also induced a large increase in microbial biomass C. As the specific activity of the ^{14}C-labeled SOM is not known, we cannot calculate the overall net C balance of the system. However, a recent study by Cardinael *et al*. (2015) suggested that straw did not induce a net loss of SOC, while many studies have shown that cereal straw can replenish SOC reserves (Liu *et al*., 2003; Malhi *et al*., 2006). In practical terms, straw still represents the most widely available feedstock for farmers and from some perspectives could be seen as a better soil conditioning agent than biochar, particularly in the short term (as it actively promotes microbial activity and nutrient cycling, promotes better aggregation and structural stability, is less susceptible to wind/water erosion, and does not have to be transported away and processed prior to field application). Based on investigations of historical charcoal burial sites, however, biochar may also promote some of these attributes in the longer term (Borchard *et al*., 2014; Hernandez-Soriano *et al*., 2016). Further, ongoing legislative, economic, and social barriers are still likely to stifle widespread adoption of biochar in many cereal production areas (Jones *et al*., 2012; Rittl *et al*., 2015b). In conclusion, biochar had a much lesser effect on the size, activity, and structure of the soil microbial community in comparison with straw and resulted in greater protection of native SOM. It is also likely that the biochar-derived C will persist for longer in soil, particularly those chars produced at high temperatures. If the sole goal is to maximize C storage in soil, then biochars produced at higher temperatures have the greatest potential; however, if other soil quality cobenefits are required, then we will still advocate the use of straw and torrefied biomass produced at low temperatures.

Acknowledgements

This study was supported by the Welsh European Funding Office, under the SEREN program, the Key Agriculture R&D Program of Guizhou Province (NY [2012]3019), and the Opening Fund of the State Key Environmental Geochemistry (SKLEG15902).

References

Al-Wabel MI, Al-Omran A, El-Naggar AH, Nadeem M, Usman ARA (2013) Pyrolysis temperature induced changes in characteristics and chemical composition of biochar produced from conocarpus wastes. *Bioresource Technology*, **131**, 374–379.

Angin D (2013) Effect of pyrolysis temperature and heating rate on biochar obtained from pyrolysis of safflower seed press cake. *Bioresource Technology*, **128**, 593–597.

Bach QV, Chen WH, Chu YS, Skreiberg O (2016) Predictions of biochar yield and elemental composition during torrefaction of forest residues. *Bioresource Technology*, **215**, 239–246.

Boddy E, Roberts P, Hill PW, Farrar J, Jones DL (2008) Turnover of low molecular weight dissolved organic C (DOC) and microbial C exhibit different temperature sensitivities in Arctic tundra soils. *Soil Biology & Biochemistry*, **40**, 1557–1566.

Borchard N, Ladd B, Eschemann S, Hegenberg D, Moseler BM, Amelung W (2014) Black carbon and soil properties at historical charcoal production sites in Germany. *Geoderma*, **232**, 236–242.

Brändli RC, Hartnik T, Henriksen T, Cornelissen G (2008) Sorption of native polyaromatic hydrocarbons (PAH) to black carbon and amended activated carbon in soil. *Chemosphere*, **73**, 1805–1810.

Brookes PC, Landman A, Pruden G, Jenkinson DS (1985) Chloroform fumigation and the release of soil nitrogen: a rapid direct extraction method to measure microbial biomass nitrogen in soil. *Soil Biology & Biochemistry*, **17**, 837–842.

Bruun S, Thomsen IK, Christensen BT, Jensen LS (2008) In search of stable soil organic carbon fractions: a comparison of methods applied to soils labelled with ^{14}C for 40 days or 40 years. *European Journal of Soil Science*, **59**, 247–256.

Buyer JS, Sasser M (2012) High throughput phospholipid fatty acid analysis of soils. *Applied Soil Ecology*, **61**, 127–130.

Cardinael R, Eglin T, Guenet B, Neill C, Houot S, Chenu C (2015) Is priming effect a significant process for long-term SOC dynamics? Analysis of a 52-years old experiment. *Biogeochemistry*, **123**, 203–219.

Cayuela ML, Sinicco T, Mondini C (2009) Mineralization dynamics and biochemical properties during initial decomposition of plant and animal residues in soil. *Applied Soil Ecology*, **41**, 118–127.

Cross A, Sohi SP (2011) The priming potential of biochar products in relation to labile carbon contents and soil organic matter status. *Soil Biology & Biochemistry*, **43**, 2127–2134.

De Nobili M, Contin M, Mondini C, Brookes PC (2001) Soil microbial biomass is triggered into activity by trace amounts of substrate. *Soil Biology & Biochemistry*, **33**, 1163–1170.

Defra (2014) *Area of Crops Grown for Bioenergy in England and the UK: 2008–2013*. Department for Environment, Food and Rural Affairs, London, UK.

Dudley RJ, Churchill PF (1995) Effect and potential ecological significance of the interaction of humic acids with two aquatic extracellular proteases. *Freshwater Biology*, **34**, 485–494.

EBC (2012) *European Biochar Certificate Guidelines for a Sustainable Production of Biochar*. European Biochar Foundation, Arbaz, Switzerland.

Farrar J, Boddy E, Hill PW, Jones DL (2012) Discrete functional pools of soil organic matter in a UK grassland soil are differentially affected by temperature and priming. *Soil Biology & Biochemistry*, **49**, 52–60.

Farrell M, Macdonald LM, Baldock JA (2015) Biochar differentially affects the cycling and partitioning of low molecular weight carbon in contrasting soils. *Soil Biology & Biochemistry*, **80**, 79–88.

Fontaine S, Bardoux G, Abbadie L, Mariotti A (2004) Carbon input to soil may decrease soil carbon content. *Ecology Letters*, **7**, 314–320.

Frostegård Å, Bååth E, Tunlid A (1993) Shifts in the structure of soil microbial communities in limed forests as revealed by phospholipid fatty acid analysis. *Soil Biology & Biochemistry*, **25**, 723–730.

Frostegård Å, Tunlid A, Bååth E (2011) Use and misuse of PLFA measurements in soils. *Soil Biology & Biochemistry*, **43**, 1621–1625.

Gaskin J, Steiner C, Harris K, Das KC, Bibens B (2008) Effect of low-temperature pyrolysis conditions on biochar for agricultural use. *Transactions of the ASABE*, **51**, 2061–2069.

Glanville HC, Hill PW, Schnepf A, Oburger E, Jones DL (2016) Combined use of empirical data and mathematical modelling to better estimate the microbial turnover of isotopically labelled carbon substrates in soil. *Soil Biology & Biochemistry*, **94**, 154–168.

Glaser B, Haumaier L, Guggenberger G *et al.* (2001) The 'Terra Preta' phenomenon: a model for sustainable agriculture in the humid tropics. *Naturwissenschaften*, **88**, 37–41.

Glaser B, Lehmann J, Zech W (2002) Ameliorating physical and chemical properties of highly weathered soils in the tropics with charcoal – a review. *Biology and Fertility of Soils*, **35**, 219–230.

Gronnow MJ, Budarin VL, Masek O *et al.* (2013) Torrefaction/biochar production by microwave and conventional slow pyrolysis – comparison of energy properties. *Global Change Biology Bioenergy*, **5**, 144–152.

Hamer U, Marschner B, Brodowski S *et al.* (2004) Interactive priming of black carbon and glucose mineralisation. *Organic Geochemistry*, **35**, 823–830.

Hernandez-Soriano MC, Kerre B, Goos P, Hardy B, Dufey J, Smolders E (2016) Long-term effect of biochar on the stabilization of recent carbon: soils with historical inputs of charcoal. *Global Change Biology Bioenergy*, **8**, 371–381.

Hill PW, Marshall C, Williams GG *et al.* (2007) The fate of photosynthetically-fixed carbon in *Lolium perenne* grassland as modified by elevated CO_2 and sward management. *New Phytologist*, **173**, 766–777.

Hill PW, Farrar JF, Jones DL (2008) Decoupling of microbial glucose uptake and mineralization in soil. *Soil Biology & Biochemistry*, **40**, 616–624.

Hill PW, Farrell M, Jones DL (2012) Bigger may be better in soil N cycling, does rapid acquisition of small L-peptides by soil microbes dominate fluxes of protein-derived N in soil? *Soil Biology & Biochemistry*, **48**, 106–112.

Hill PW, Garnett MH, Farrar JF (2015) Living roots magnify the response of soil organic carbon decomposition to temperature in temperate grassland. *Global Change Biology*, **21**, 1368–1375.

Jiang XY, Denef K, Stewart CE, Cotrufo MF (2016) Controls and dynamics of biochar decomposition and soil microbial abundance, composition, and carbon use efficiency during long-term biochar-amended soil incubations. *Biology and Fertility of Soils*, **52**, 1–14.

Joergensen RG, Wu J, Brookes PC (2011) Measuring soil microbial biomass using an automated procedure. *Soil Biology and Biochemistry*, **43**, 873–876.

Jones DL, Kemmitt SJ, Wright D, Cuttle SP, Bol R, Edwards AC (2005) Rapid intrinsic rates of amino acid biodegradation in soils are unaffected by agricultural management strategy. *Soil Biology & Biochemistry*, **37**, 1267–1275.

Jones DL, Murphy DV, Khalid M, Ahmad W, Edwards-Jones G, DeLuca TH (2011) Short-term biochar-induced increase in soil CO_2 release is both biotically and abiotically mediated. *Soil Biology & Biochemistry*, **43**, 1723–1731.

Jones DL, Rousk J, Edwards-Jones G, DeLuca TH, Murphy DV (2012) Biochar-mediated changes in soil quality and plant growth in a three year field trial. *Soil Biology & Biochemistry*, **45**, 113–124.

Keiblinger KM, Hall EK, Wanek W *et al.* (2010) The effect of resource quantity and resource stoichiometry on microbial carbon-use-efficiency. *FEMS Microbiology Ecology*, **73**, 430–440.

Koelamans AA, Meulman B, Meijer T, Jonker MTO (2009) Attenuation of polychlorinated biphenyl sorption to charcoal by humic acids. *Environmental Science and Technology*, **43**, 736–742.

Kuzyakov Y, Friedel JK, Stahr K (2000) Review of mechanisms and quantification of priming effects. *Soil Biology & Biochemistry*, **32**, 1485–1498.

Lehmann J (2007) A handful of carbon. *Nature*, **447**, 143–144.

Lehmann J, Gaunt J, Rondon M (2006) Bio-char sequestration in terrestrial ecosystems – a review. *Mitigation and Adaptation Strategies for Global Change*, **11**, 395–419.

Liang B, Lehmann J, Sohi SP *et al.* (2010) Black carbon affects the cycling of non-black carbon in soil. *Organic Geochemistry*, **41**, 206–213.

Liu XB, Han XZ, Song CY, Herbert SJ, Xing BS (2003) Soil organic carbon dynamics in black soils of China under different agricultural management systems. *Communications in Soil Science and Plant Analysis*, **34**, 973–984.

Lu W, Ding W, Zhang J (2014) Biochar suppressed the decomposition of organic carbon in a cultivated sandy loam soil: a negative priming effect. *Soil Biology & Biochemistry*, **76**, 12–21.

Luo Y, Durenkamp M, De Nobili M, Lin Q, Brookes PC (2011) Short term soil priming effects and the mineralisation of biochar following its incorporation to soils of different pH. *Soil Biology and Biochemistry*, **43**, 2304–2314.

Maestrini B, Nannipieri P, Abiven S (2015) A meta-analysis on pyrogenic organic matter induced priming effect. *Global Change Biology Bioenergy*, **7**, 577–590.

Malhi SS, Lemke R, Wang ZH, Chhabra BS (2006) Tillage, nitrogen and crop residue effects on crop yield, nutrient uptake, soil quality, and greenhouse gas emissions. *Soil & Tillage Research*, **90**, 171–183.

Marris E (2006) Putting the carbon back: black is the new green. *Nature*, **442**, 624–626.

Mathews JA (2008) Carbon-negative biofuels. *Energy Policy*, **36**, 940–945.

McClellan AT, Deenik J, Uehara G, Antel M (2007) Effects of flashed carbonized macadamia nutshell charcoal on plant growth and soil chemical properties. The ASA-CSSA-SSSA International Annual Meeting, November 4–8, 2007, New Orleans, LA, ASA-CSSA-SSSA, Wisconsin, USA.

Méndez A, Tarquis A, Saa-Requejo A, Guerrero F, Gasco G (2013) Influence of pyrolysis temperature on composted sewage sludge biochar priming effect in a loamy soil. *Chemosphere*, **93**, 668–676.

Miranda KM, Espey MG, Wink DA (2001) A rapid, simple spectrophotometric method for simultaneous detection of nitrate and nitrite. *Nitric Oxide Biology and Chemistry*, **5**, 62–71.

Monti A, Di Virgilio N, Venturi G (2008) Mineral composition and ash content of six major energy crops. *Biomass and Bioenergy*, **32**, 216–223.

Mukherjee A, Zimmerman AR, Harris W (2011) Surface chemistry variations among a series of laboratory-produced biochars. *Geoderma*, **163**, 247–255.

Mulvaney R (1996) Nitrogen-inorganic forms. In: *Methods of Soil Analysis. Part 3. Chemical Methods* (ed. Sparks DL), pp. 1123–1184. SSSA, Madison, WI, USA.

Murphy J, Riley JP (1962) A modified single solution method for the determination of phosphate in natural waters. *Analytica Chimica Acta*, **27**, 31–36.

Murphy CJ, Baggs EM, Morley N, Wall DP, Paterson E (2015) Rhizosphere priming can promote mobilisation of N-rich compounds from soil organic matter. *Soil Biology & Biochemistry*, **81**, 236–243.

Ni JZ, Pignatello JJ, Xing BS (2011) Adsorption of aromatic carboxylate ions to black carbon (biochar) is accompanied by proton exchange with water. *Environmental Science & Technology*, **45**, 9240–9248.

Oburger E, Glanville H, Rousk J, Golyshin P, Jones DL (2012) Mineralisation of low molecular weight carbon substrates in soil solution under laboratory and field conditions. *Soil Biology & Biochemistry*, **48**, 88–95.

Riedel T, Iden S, Geilich J, Wiedner K, Durner W, Biester H (2014) Changes in the molecular composition of organic matter leached from an agricultural topsoil following addition of biomass-derived black carbon (biochar). *Organic Geochemistry*, **69**, 52–60.

Rittl TF, Novotny EH, Balieiro FC, Hoffland E, Alves BJR, Kuyper TW (2015a) Negative priming of native soil organic carbon mineralization by oilseed biochars of contrasting quality. *European Journal of Soil Science*, **66**, 714–721.

Rittl TF, Arts B, Kuyper TW (2015b) Biochar: an emerging policy arrangement in Brazil? *Environmental Science & Policy*, **51**, 45–55.

Sinsabaugh RL, Manzoni S, Moorhead DL, Richter A (2013) Carbon use efficiency of microbial communities: stoichiometry, methodology and modelling. *Ecology Letters*, **16**, 930–939.

Smith JL, Collins HP, Bailey VL (2011) The effect of young biochar on soil respiration. *Soil Biology & Biochemistry*, **42**, 2345–2347.

Spohn M, Potsch EM, Eichorst SA, Woebken D, Wanek W, Richter A (2016) Soil microbial carbon use efficiency and biomass turnover in a long-term fertilization experiment in a temperate grassland. *Soil Biology & Biochemistry*, **97**, 168–175.

Spokas KA, Reicosky DC (2009) Impacts of sixteen different biochars on soil greenhouse gas production. *Annals of Environmental Science*, **3**, 179–193.

Subedi R, Kammann C, Pelissetti S, Taupe N, Bertora C, Monaco S, Grignani C (2015) Does soil amended with biochar and hydrochar reduce ammonia emissions following the application of pig slurry? *European Journal of Soil Science*, **66**, 1044–1053.

Tian J, Miller V, Chiu PC, Maresca JA, Guo MX, Imhoff PT (2016) Nutrient release and ammonium sorption by poultry litter and wood biochars in stormwater. *Science of the Total Environment*, **553**, 596–606.

Tiemann LK, Billings SA (2011) Changes in variability of soil moisture alter microbial community C and N resource use. *Soil Biology & Biochemistry*, **43**, 1837–1847.

Wang Y, Hu Y, Zhao X, Wang SQ, Xing GX (2013) Comparisons of biochar properties from wood material and crop residues at different temperatures and residence times. *Energy & Fuels*, **27**, 5890–5899.

Wang JY, Xiong ZQ, Kuzyakov Y (2016) Biochar stability in soil: meta-analysis of decomposition and priming effects. *Global Change Biology Bioenergy*, **8**, 512–523.

Wardle DA, Nilsson MC, Zackrisson O (2008) Fire-derived charcoal causes loss of forest humus. *Science*, **320**, 629.

Wu J, Joergensen R, Pommerening B, Chaussod R, Brookes PC (1990) Measurement of soil microbial biomass C by fumigation-extraction – an automated procedure. *Soil Biology & Biochemistry*, **22**, 1167–1169.

Yuan JH, Xu RK, Zhang H (2011) The forms of alkalis in the biochar produced from crop residues at different temperatures. *Bioresource Technology*, **102**, 3488–3497.

Yuan H, Lu T, Wang Y, Huang HY, Chen Y (2014) Influence of pyrolysis temperature and holding time on properties of biochar derived from medicinal herb (*Radix isatidis*) residue and its effect on soil CO_2 emission. *Journal of Analytical and Applied Pyrolysis*, **110**, 277–284.

Zimmerman AR (2010) Abiotic and microbial oxidation of laboratory-produced black carbon (biochar). *Environmental Science and Technology*, **44**, 1295–1301.